



# Ventilator-associated pneumonia diagnosis: electrochemical sensors for rapid and sensitive detection of *pyocyanin*

Mohammad Noorizadeh<sup>1</sup> · Tamim M. Al-Hasan<sup>1</sup> · Mizaj S. Sha<sup>2</sup> · Faycal Bensaali<sup>1</sup> · Nader Meskin<sup>1</sup> · Kishor K. Sadasivuni<sup>2</sup> · Susu M. Zughaier<sup>3</sup> · Mahmoud Elgamal<sup>3</sup> · Ali Ait Hssain<sup>4</sup>

Received: 26 November 2023 / Accepted: 13 March 2024  
© The Author(s) 2024

## Abstract

Ventilator-associated pneumonia (VAP) is a severe condition in critically ill patients that requires timely diagnosis to improve patient outcomes. In this study, we developed an electrochemical sensor for *pyocyanin* detection using a TiO<sub>2</sub>-NiO-rGO catalyst and found that it could detect the concentration of *pyocyanin* required for mimicking the throat trachea's environment (LOD: 0.2 µg/mL). We also investigated using DNA aptamer for detecting *pyocyanin*, a biomarker of *Pseudomonas aeruginosa*, a common causative agent of VAP. Our findings suggest that the TiO<sub>2</sub>-NiO-rGO catalyst without aptamer could provide a rapid and cost-effective diagnostic tool for VAP, and the electrochemical sensor has the potential to be made disposable for *in vivo* applications. Using the TiO<sub>2</sub>-NiO-rGO catalyst offers synergistic effects that enhance the detection process's overall electrochemical performance, sensitivity, and selectivity. This work's results demonstrate that electrochemical detection of *pyocyanin* using a TiO<sub>2</sub>-NiO-rGO catalyst holds great potential for various applications, such as clinical diagnostics and drug discovery. Further research and optimization of the catalyst composition, morphology, and surface modifications can contribute to advancing this *pyocyanin* electrochemical detection approach.

**Keywords** Biosensors · Bio-signal processing · DNA aptamer · Electrochemistry · Nosocomial infections · Ventilator-associated pneumonia (VAP)

## 1 Introduction

Ventilator-associated pneumonia (VAP) is a prevalent health-care-associated infection that mostly affects critically ill patients on mechanical ventilation (MV) for more than 48 hours [1, 2]. Up to 28% of patients undergoing MV in the intensive care unit (ICU) are at risk of developing VAP, making it the most common nosocomial infection [3, 4]. VAP constitutes a significant portion of nosocomial infections in ICUs, with a majority of them (around 83% of the cases) associated with MV [5]. VAP's most prevalent pathogens include *Acinetobacter baumannii*, *Klebsiella pneumoniae*, methicillin-resistant *Staphylococcus aureus* (MRSA), *Staphylococcus aureus*, and *Pseudomonas aeruginosa* [6].

VAP is a severe condition that increases the mortality risk by 2–10 times and prolongs the duration of MV and hospitalization [7]. Patients who have a significant amount of *P. aeruginosa* colonization are more likely to experience higher mortality rates in comparison to those who have been infected by other pathogens [8, 9].

Methods currently used for diagnosing VAP involve clinical observations, such as fever and purulent secretion, chest radiography, as well as monitoring oxygenation levels [10–12], and microbiological testing of sputum samples. However, these methods have several limitations in predicting patient outcomes and are often time-consuming [13–15]. False-negative results are common with microbiological testing of sputum samples, particularly when patients undergo antibiotic treatment [16, 17]. Consequently, unspecific diagnoses based on clinical criteria often have a 2–4 fold lower incidence rate compared to overnight microbiological testing [16, 17]. Bronchoscopy sampling can improve diagnostic accuracy, but it is an invasive procedure with a prolonged culturing duration [15]. To rapidly respond to microbial infections, it is typical for patients in the ICU to

Tamim M. Al-Hasan, Mizaj S. Sha, Faycal Bensaali, Nader Meskin, Kishor K. Sadasivuni, Susu M. Zughaier, Mahmoud Elgamal and Ali Ait Hssain contributed equally to this work.

✉ Mohammad Noorizadeh  
m.noorizadeh@qu.edu.qa

Extended author information available on the last page of the article

receive broad-spectrum antibiotics [18–20]. However, this practice contributes to developing antibiotic resistance due to selective pressure after resistance has emerged [21–23]. Therefore, alternative and non-invasive methods for detecting VAP in ICU patients are urgently needed, which utilize alternative markers of pulmonary infections [24]. VAP incurs a high financial burden, with hospital expenses per patient reaching approximately \$39,500 [25, 26].

Various methods have been employed to improve the detection of volatile organic compounds (VOCs) associated with VAP. With the recent advances in the areas of sensors and medical practice, numerous studies have aimed at enhancing the methods of detecting VOCs. These studies have included methods using electronic-chemical sensors and pattern recognition systems [27–30] that can detect different odors (e-nose) [31] to detect VAP [32, 33], and those that utilize computer vision for fast detection of VAP or other pathologies using medically obtained results such as the log of breathprints, computed tomography scans, magnetic resonance imaging, or X-ray [34–37]. Moreover, secondary bacterial infections frequently occur in individuals with severe COVID-19 and influenza, particularly among hospitalized patients requiring intubation and MV [38]. Among these cases, bacterial pneumonia is the predominant cause of mortality. Notably, *P. aeruginosa*, a bacterium known for its production of *pyocyanin*, is a significant contributor to VAP, a prevalent secondary bacterial infection in such clinical contexts [39, 40]. However, the trend of using biosensors in VAP detection has become more prominent in recent years, especially with the outbreak of the COVID-19 pandemic

[41, 42], and they have been used for a considerable time to detect other VOCs related to lung pathologies [41–45]. Further details of some significant studies on this topic can be seen in Table 1.

DNA aptamers are short single-stranded DNA sequences that can bind to target molecules with high specificity and affinity. They have several advantages over traditional antibodies, including lower cost, ease of synthesis, and improved stability. Previous studies have shown that DNA aptamer can detect various pathogens, including *P. aeruginosa*, the most common pathogen associated with VAP. Therefore, there is a rationale for using DNA aptamers as diagnostic tools for VAP.

This study describes the development of an electrochemical sensor for rapidly detecting *pyocyanin*. As part of a larger diagnostic system, this sensor has the potential to provide rapid and early detection of VAP, enabling timely interventions and improved patient outcomes, since *P. aeruginosa* is electrochemically active [55]. It will be integrated into the diagnostic system for *in vivo* detection of VAP, which could provide early warning signs for the disease, as illustrated in Fig. 1. We aim to evaluate the sensitivity and selectivity of the electrochemical sensor in detecting the virulence factor produced by *P. aeruginosa* with and without using aptamer. It is shown that the TiO<sub>2</sub>-NiO-rGO catalyst without aptamer provides a rapid and cost-effective diagnostic tool for VAP.

Our study shows that using the proposed electrochemical sensor as a diagnostic tool for VAP could lead to improved patient outcomes and reduced healthcare costs. The developed sensor has a very rapid response.

**Table 1** Overview of previous studies for detecting microbial pathologies

Pathology	Biomarker	Material/Method	LOD	Ref.
COPD	ILK-6	LIGMA-FET	1.37 pg/mL	[43]
	ILK-6	OECT	0.2 ng/mL	[44]
	ILK-6	G-FET	0.012 nM	[45]
COVID-19	SPR	G-FET	0.001 pg/mL	[41]
	SPR	G-FET	200 fM	[42]
Influenza	DNA	rGO	5 pM	[46]
	DNA aptamer	GO	1 ng/mL	[47]
	SGP	G-FET	130 pM	[48]
VAP	PYC	Carbon	0.14 μM	[49]
	PYC	AuZF	25 μM	[50]
	PYC	Carbon ink	95 nM	[51]
	PYC	SERS	5 ppb	[52]
	PYC	AdSV	2 nM	[53]
	PYC	Gold Nanoparticles	500 nM	[54]

**Table Key:** *AdSV* Adsorptive Stripping Voltammetric, *AuZF* Gold-coated Zein Film, *G-FET* Graphene-based Field-Effect Transistor, *ILK-6* Interleukin-6, *LIGMA-FET* Liquid Immunosensor Gate for Medical Assistive Field-Effect Transistor, *OECT* Organic Electro-Chemical Transistor, *PYC* Pyocyanin, *SGP* Sialylglycopeptide, *SPR* Spike Protein, *SERS* Surface-enhanced Raman Spectroscopy

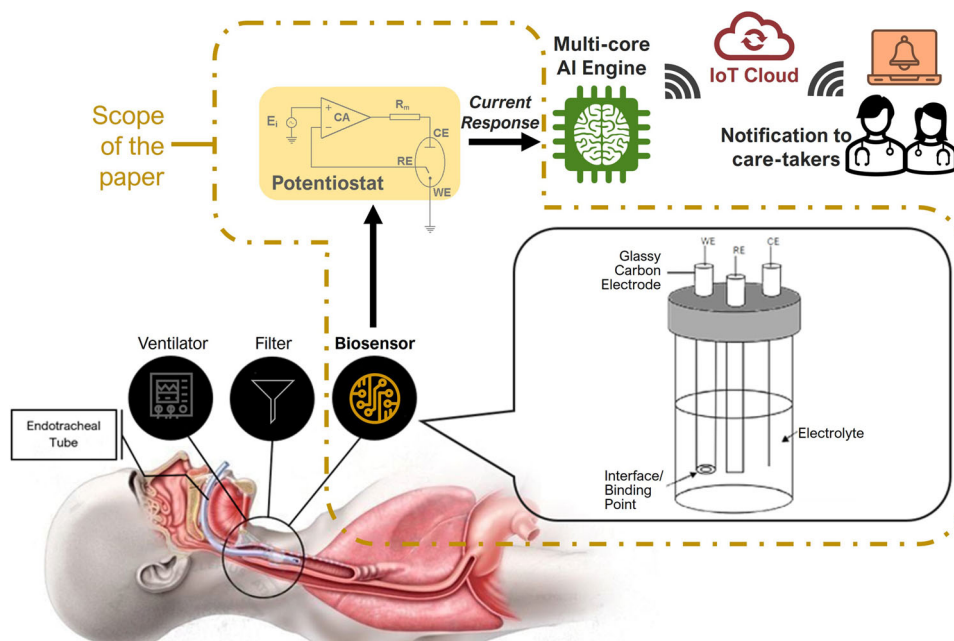


**Fig. 1** Schematic diagram of the overall proposed system for *in vivo* diagnosis of VAP and other lung pathologies

## 2 Materials and methodology

### 2.1 Chemicals

Acetylene black (ACET), N-Methyl-2-pyrrolidone (NMP), and nickel nitrate were purchased from SRL. Polyvinylidene difluoride (PVDF), Nafion, ethanol, glacial acetic acid, and graphite were purchased from Rankem, India. 100 nmol ssDNA aptamer (5'-CTT CTG CCC GCC TCC TTC CTA GCC GGA TCG CGC TGG CCA GAT GAT ATA AAG GGT CAG CCC CCC AGG AGA CGA GAT AGG CGG ACA CT-3') was purchased from Integrated DNA Technologies, Belgium. Finally, *pyocyanin* [CAS85-66-5/ref.10009594] was purchased from Cayman Chemicals, Estonia. The chemicals were used in their original form without any alterations. All reagents were synthesized using deionized (DI) water. For electrochemical experiments, glassy carbon electrodes from Sigma Aldrich were used. Glassy carbon electrodes (GCEs) are chemically electrochemically inert and relatively reproducible.

### 2.2 Synthesis of nanocomposite

#### 2.2.1 Synthesis of TiO<sub>2</sub>-NiO nanoparticles

A sol-gel method was used to create TiO<sub>2</sub>-NiO nanoparticles. First, 50 mL of ethanol was mixed with 5.7 mL of titanium isopropoxide. Once thoroughly blended, a mixture of 3 g of aqueous Ni(NO<sub>3</sub>)<sub>2</sub>·2H<sub>2</sub>O 14 mL of DI water was introduced. Following this, stirring was discontinued until the solution

solidified into a gel-like substance. The gel was left to age naturally for 5 hours before being dried at 80°C for 48 hours. The next step involved calcining the dried gel at 300°C for 2 hours to produce TiO<sub>2</sub>-NiO.

#### 2.2.2 Synthesis of TiO<sub>2</sub>-NiO-rGO nanoparticles

The modified Hummer process created graphene oxide (GO) by oxidizing graphite [56]. The solvothermal method was used to reduce GO to rGO [56]. The mixture is then heated at different temperatures for the reduction process. Initially, 200 mg of GO was combined with 10 mL of DI water and 20 mL C<sub>2</sub>H<sub>5</sub>OH by subjecting the mixture to intense sonication for 30 minutes. A stable GO dispersion was obtained and brought to a Teflon-lined stainless-steel autoclave with a capacity of 80 mL. The mixture was then heated at 150°C for 2 hours. A sol-gel method was used to create TiO<sub>2</sub>-NiO nanoparticles. First, 50 mL of ethanol was mixed with 5.7 mL of acetic acid. Once thoroughly blended, a mixture of 3 g of aqueous Ni(NO<sub>3</sub>)<sub>2</sub>·2H<sub>2</sub>O 14 mL of DI water was introduced into the blend. Following this, stirring was discontinued until the solution solidified into a gel-like substance. The gel was left to age naturally for 5 hours before being dried at 80°C for 48 hours. The next step involved calcining the dried gel at 300°C for 2 hours to produce TiO<sub>2</sub>-NiO. To create the solution, 0.04 g of rGO was mixed in 1.5 mL of NMP via ultrasonic homogenization. The resulting solution was then uniformly mixed with 0.35 g of TiO<sub>2</sub>-NiO, 0.05 g of PVDF, and 0.05 g of ACET. The two solutions were mixed at 80°C for 12 hours to get a black slurry. Then it was dried for 12 hours at 120°C [57].

### 2.3 Fabrication of electrode

The catalytic ink was prepared by sonicating 15 mg of the nanocomposite in an ice bath for 2 hours with 20  $\mu\text{L}$  of Nafion and 1.5 mL of ethanol. Following sonication, 10  $\mu\text{L}$  of the catalytic ink was placed on 2 mm diameter glassy carbon electrodes (GCE) and allowed to dry at room temperature.

### 2.4 Characterization of catalyst

The X-ray diffractometer (XRD-6100, LabX, SHIMADZU Ltd., Japan) was used to obtain the crystal phases. Transmission electron microscopy (TEM) investigated the morphology of the nanocomposite.

### 2.5 Preparation of aptamer and *pyocyanin* solutions for electrochemical assay

To prepare the aptamer and *pyocyanin* solutions, the aptamer was initially re-suspended and folded into its tertiary structure for optimal binding. The aptamer storage tube was briefly centrifuged to ensure the dried aptamer pellet was at the bottom of the tube. The pellet was then re-suspended in TE buffer (10 mM Tris HCl, 0.1 mM EDTA, pH 7.5), nuclease-free water, to achieve a 100  $\mu\text{M}$  concentration. After incubating the solution at room temperature for 30 minutes, the tube was vortexed for 20 seconds and then centrifuged for 1 minute according to the aptamer preparation protocol. The re-suspended DNA was aliquoted and stored at  $-20^{\circ}\text{C}$ .

Next, for diluting the aptamer, 95  $\mu\text{L}$  of molecular grade water (MGW) is added to a sample of the 5  $\mu\text{L}$  aptamer to achieve a final volume of 100  $\mu\text{L}$ . This solution will have a concentration of 10  $\mu\text{M}$  for the stock solution. After prepar-

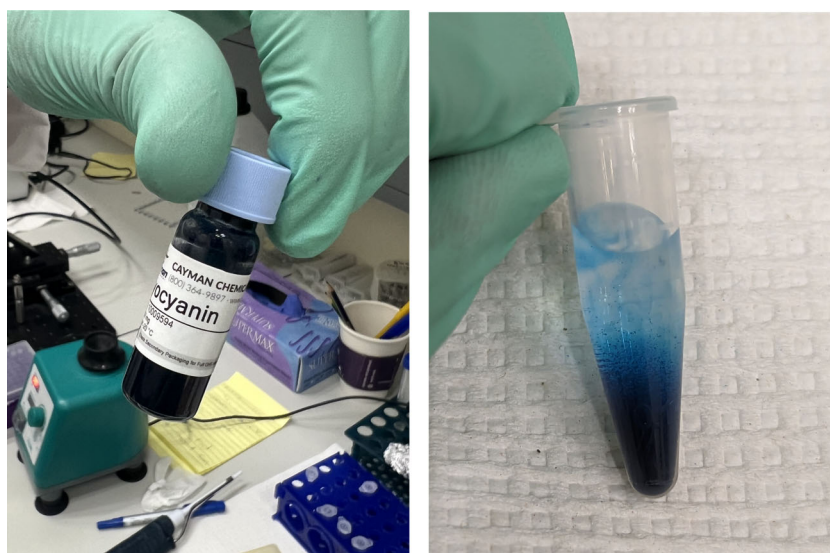
ing the stock solution, the working solution for the aptamer can be prepared by diluting 10  $\mu\text{L}$  of the stock solution with 90  $\mu\text{L}$  of MGW. This results in a final concentration of 2  $\mu\text{M}$  for the working solution. Similarly, the preparation of *pyocyanin* working and stock solutions was performed. Initially, 50 mg of *pyocyanin* was dissolved in 2 mL MGW to obtain the stock solution. To prepare the 1 mg/mL working stock solution, 40  $\mu\text{L}$  of the stock solution was added to 960  $\mu\text{L}$  of MGW. To prepare the working solution of 0.1667 mg/mL concentration to mimic the throat trachea's environment, 200  $\mu\text{L}$  of the 1 mg/mL *pyocyanin* solution was mixed with 1 mL of MGW. This resulted in the desired concentration of *pyocyanin* as shown in Fig. 2, which can be further used for downstream assays and experiments.

### 2.6 Electrochemical experiments

Various electrochemical experiments, including cyclic voltammetry (CV), chronoamperometry, and electrochemical impedance (EIS), were carried out using a Gamry galvanostat (Ref 600). Herein, a catalytic ink-coated GC working electrode, an Ag/AgCl reference electrode, and a graphite rod counter electrode were used. *Pyocyanin* was detected by employing 25 mL of 0.5 M KOH electrolyte, resulting in a final concentration of 0.2  $\mu\text{g}/\text{mL}$ . The measurements were conducted at specific parameters while varying the swept rates between 50 and 200 mV/s. All electrochemical experiments were carried out at ambient conditions.

Using nuclease-free water to prepare DNA aptamers and using deionized water during the electrochemistry experiment is generally not a problem. Both types of water serve different purposes and are suitable for their respective stages in the experimental process. DNA aptamers are short single-

**Fig. 2** Preparing the *pyocyanin* with concentration of 0.1667 mg/mL



(a)

(b)

stranded DNA molecules selected for their specific binding affinity to a target molecule. Nuclease-free water is crucial during the preparation of DNA aptamers to ensure that nucleases do not degrade the DNA molecules and helps maintain the integrity and stability of the DNA aptamers during preparation. Nucleases could potentially degrade the DNA aptamers, compromising their functionality and affecting the experiments' accuracy and reliability. Electrochemical analysis often involves sensitive measurements of electrical properties, particularly in the context of DNA aptamers, which are used as bio-recognition elements in biosensors. Deionized water creates a controlled ionic environment during the electrochemistry experiment. It has a low ion concentration, minimizing interference with the electrochemical measurements and helping to maintain a consistent and controlled baseline for the experiment. Starting with nuclease-free water for DNA aptamer preparation ensures the quality and integrity of the aptamer molecules. Subsequently, during the electrochemistry experiment, deionized water maintains the desired ionic environment essential for accurate electrochemical measurements. There's no inherent conflict or problem in using nuclease-free water for aptamer preparation and deionized water during the electrochemical analysis, as they serve distinct purposes in the experiment.

### 3 Results and discussion

#### 3.1 Structural and morphological assessment

Figure 3 displays the XRD patterns. The TiO<sub>2</sub> nanoparticles exhibited peaks at 2θ of 24.5°, 47°, 54.1°, and 63.7° corresponding to (101), (200), (211) and (204) plane respectively (JCPDS Card No. 21-1272). The presence of NiO at 36.9°, 62.8°, and 75.4° in composite indicated a hexagonal plane

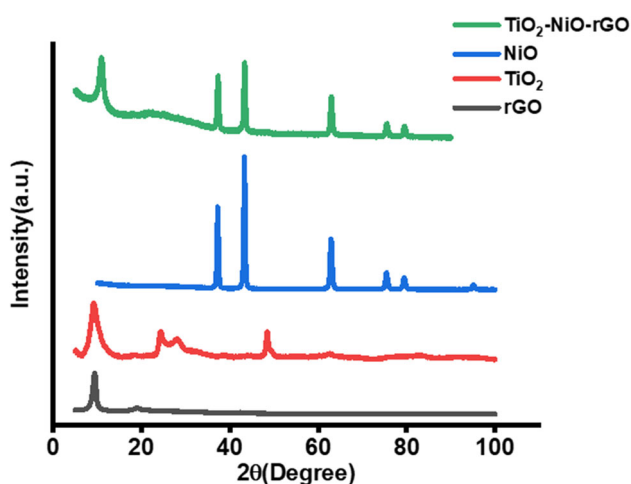


Fig. 3 XRD pattern

(111), (220) and (222), respectively (JCPDS Card No. 73-1523) [58]. A few peaks on the rGO surface suggested that the carbonaceous surface had been well-exfoliated and was covered by other metal oxides [59, 60]. Diffraction peaks of TiO<sub>2</sub>-NiO-rGO were sharper, indicating the crystalline nature.

The TEM analysis (Fig. 4) of the composite confirms the formation of the nanocomposite, with *d* values of 0.26 nm, 0.25 nm, and 0.34 nm obtained for the rGO, NiO, and TiO<sub>2</sub> nanoparticles, which are attributed to the (002) of rGO, (111) of NiO, and (101) of TiO<sub>2</sub> respectively. The TEM images indicate the presence of NiO and rGO nanoparticles in the inner layer at the interface and the TiO<sub>2</sub> nanoparticles in the outer layer.

#### 3.2 Electrochemical profile for detection of pyocyanin

Initially, the efficiency of GCE in detecting *pyocyanin* was determined by CV. Initially, the experiments were carried out with and without adding *pyocyanin* (Fig. 5a). It was observed that GCE failed to detect *pyocyanin*. Then, CV analysis was carried out using TiO<sub>2</sub>-NiO-rGO coated GCE. In the first case, analysis was performed without *pyocyanin*. In the second case, *pyocyanin* was added. In the third case, aptamer and *pyocyanin* were added (Fig. 5b). The results showed that cyclic voltammograms of TiO<sub>2</sub>-NiO-rGO had more area and distinct oxidation and reduction peaks in detecting *pyocyanin* in the absence of aptamer.

Figure 6a shows the CV measured during *pyocyanin* detection by TiO<sub>2</sub>-NiO-rGO in KOH at different scan rates (50 to 200 mV/s). A gradual redox peak current density elevation is observed during reductions, as shown in Fig. 6a. Both Fig. 6b and c show the relation between the square root of scan rates and the peak current densities of the TiO<sub>2</sub>-NiO-rGO. It was observed that current density also increases as the scan rate increases [61]. The linear regression equation of oxidation peak current for detecting *pyocyanin* is

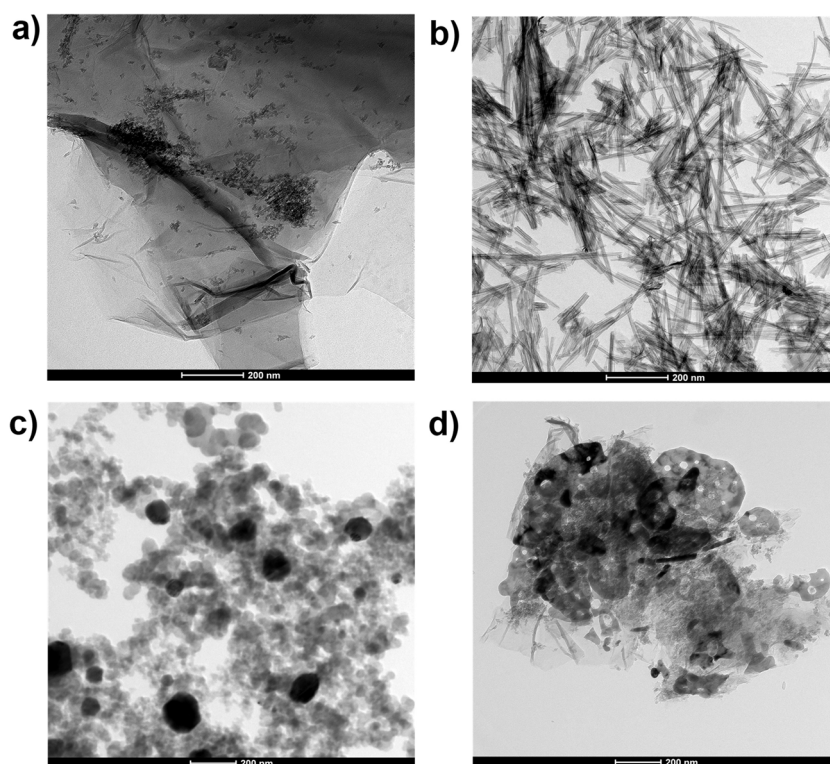
$$j \text{ (mA cm}^{-2}\text{)} = (0.5517 \pm 0.0796)x - (3.4446 \pm 0.8535), \\ R^2 = 0.9412 \quad (1)$$

Whereas the linear regression equation of reduction peak current for detecting *pyocyanin* is

$$j \text{ (mA cm}^{-2}\text{)} = (-0.6467 \pm 0.0597)x + (4.4363 \pm 0.6402), \\ R^2 = 0.9412 \quad (2)$$

where *x* in both Eq. 1 and Eq. 2 stand for the square root of scan rate, *v*<sup>1/2</sup> (Fig. 6b and c). Further, durability assessments

**Fig. 4** The TEM images of (a) rGO, (b) TiO<sub>2</sub>, (c) NiO, and (d) TiO<sub>2</sub>-NiO-rGO nanocomposite



for *pyocyanin* detection by TiO<sub>2</sub>-NiO-rGO were carried out by chronoamperometry for 10 hours at a reduction potential of  $-0.3$  V (Fig. 6d). Interestingly, TiO<sub>2</sub>-NiO-rGO reveals a much higher retention of the current even after 10 hours, indicating greater stability. Metal dissolution was not observed in the initial hour of electrolysis. However, after 4 hours of electrolysis, a small amount of TiO<sub>2</sub>-NiO-rGO was detected in the electrolyte, which was found to be only 2 wt% of the fresh electrode.

Electrochemical impedance spectroscopy (EIS) data were collected at 1.23 Vs. Ag/AgCl in the 0.1 Hz–100 kHz sweeping frequency range. EIS provides useful insights into the interfacial processes at the electrode surface by measuring the impedance response to an applied AC voltage over various frequencies. The blank electrode's  $R_{ct}$  was 695, whereas the  $R_{ct}$  of the TiO<sub>2</sub>-NiO-rGO electrode was 468. The TiO<sub>2</sub>-

NiO-rGO electrode has a lower diffusion impedance in its linear section at lower frequencies than the blank electrode combinations. This suggests the diffusion process proceeded with less resistance, enhancing ion transport from the bulk to the electrode surface. Figure 7 shows that TiO<sub>2</sub>-NiO-rGO electrodes have more electron conduction channels and reactive surfaces, leading to better electrolyte diffusion.

The electrochemical detection of *pyocyanin* using a catalyst composed of TiO<sub>2</sub>, NiO, and rGO is a promising approach that combines the advantages of each component for sensitive and selective detection of *pyocyanin* in various samples [62]. Titanium dioxide (TiO<sub>2</sub>) is a widely used semiconductor material known for its high photocatalytic activity, stability, and biocompatibility. Nickel oxide (NiO) is a transition metal oxide with excellent electrochemical properties, including high catalytic activity and good electrical

**Fig. 5** CV analysis using (a) Blank GCE, and (b) TiO<sub>2</sub>-NiO-rGO coated electrode

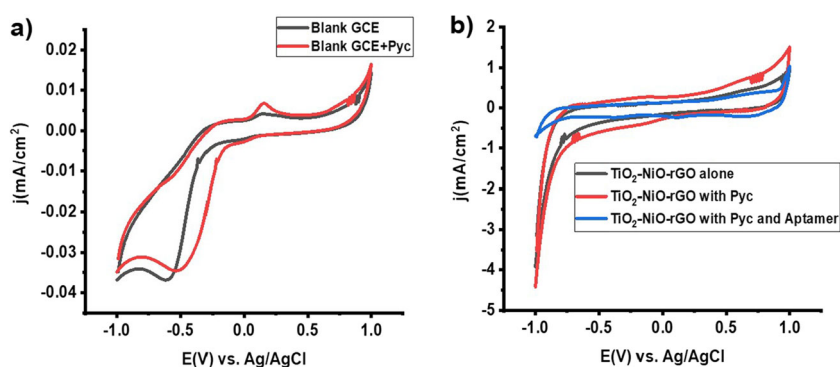
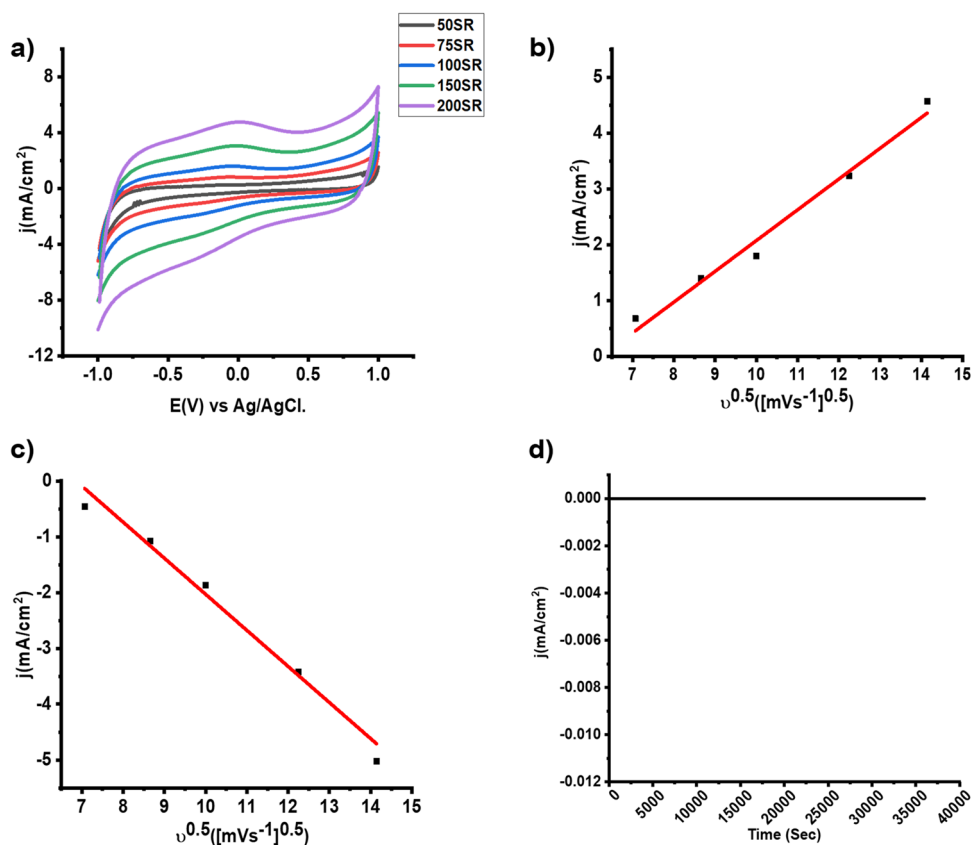


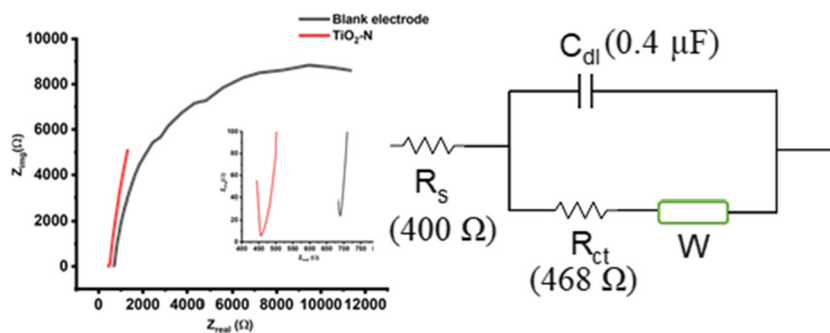
**Fig. 6** (a) CV curves at different scan rates (b) Plot of anodic peak current density against the square root of the scan rate (c) Plot of cathodic peak current density against the square root of the scan rate. (d) Durability assessments for *pyocyanin* detection



conductivity. Reduced graphene oxide (rGO) is a form of graphene that has been chemically reduced from graphene oxide, resulting in a highly conductive and stable material. The TiO<sub>2</sub>-NiO-rGO catalyst offers several benefits for electrochemical *pyocyanin* detection. First, the TiO<sub>2</sub> component provides a large surface area for *pyocyanin* adsorption and enhances the electron transfer process. Second, the NiO component acts as a catalyst, promoting *pyocyanin*'s electrochemical oxidation and reduction. Third, the rGO component serves as a conductive matrix, improving the overall electrical conductivity of the catalyst and facilitating electron transfer. The electrochemical detection of *pyocyanin* using the TiO<sub>2</sub>-NiO-rGO catalyst typically involves the adsorption of *pyocyanin* onto the catalyst surface, followed by

its electrochemical oxidation and reduction, which result in changes in electrical current that can be measured to determine the concentration of *pyocyanin* in the sample solution. The TiO<sub>2</sub>-NiO-rGO catalyst enhances the sensitivity and selectivity of the detection process, making it suitable for various applications, such as environmental monitoring, clinical diagnostics, and drug discovery. However, further research and optimization are still needed to fine-tune the catalyst composition, morphology, and surface modifications to achieve even better performance for *pyocyanin* detection. Additionally, the stability and reproducibility of the TiO<sub>2</sub>-NiO-rGO catalyst in real-world sample matrices need to be further investigated. Nevertheless, the electrochemical detection of *pyocyanin* using the TiO<sub>2</sub>-NiO-rGO catalyst

**Fig. 7** EIS spectra of TiO<sub>2</sub>-NiO-rGO and blank electrodes



holds great promise as a sensitive and selective method for detecting *pyocyanin*, contributing to the advancing analytical techniques for *pyocyanin* analysis in various fields. Therefore, the electrochemical detection of *pyocyanin* using the TiO<sub>2</sub>-NiO-rGO catalyst offers a promising approach for the accurate and sensitive detection of VAP. With further research and optimization, this method could be expanded to cover other pathogens biomarkers and further developed as a valuable tool for diagnosing and treating VAP, ultimately contributing to improved patient outcomes and better management of respiratory infections.

While the electrochemical detection of *pyocyanin* with TiO<sub>2</sub>-NiO-rGO nanocomposite represents a promising improvement in biosensing technology, it is not without obstacles. Despite the improved sensitivity and selectivity due to the synergistic effects of the composite materials, the practical implementation of this detection approach may be limited by cost, stability, and specificity. The synthesis and fabrication methods of generating nanocomposite materials may be difficult and expensive, possibly limiting their availability for general application, particularly in resource-constrained contexts. Furthermore, guaranteeing the nanocomposite's long-term stability and minimizing interference from other compounds found in complicated samples are key factors for accurate and reproducible detection. Addressing these issues through additional research and development efforts to optimize the synthesis process, increase stability, and boost specificity will be critical in realizing the full potential of electrochemical *pyocyanin* detection employing TiO<sub>2</sub>-NiO-rGO nanocomposite.

## 4 Conclusion

In conclusion, the electrochemical detection of *pyocyanin* using a catalyst composed of TiO<sub>2</sub>, NiO, and rGO is a promising approach for the sensitive and selective detection of *pyocyanin* in various samples. The TiO<sub>2</sub>-NiO-rGO catalyst provides a conductive and catalytically active surface that enables the electrochemical oxidation and reduction of *pyocyanin*, leading to changes in electrical current that can be measured to determine the *pyocyanin* concentration in the sample solution. Using TiO<sub>2</sub>, NiO nanoparticles, and rGO in the catalyst offers synergistic effects that enhance the detection process's overall electrochemical performance, sensitivity, and selectivity. This work observed that the TiO<sub>2</sub>-NiO-rGO catalyst could detect 0.2 µg/mL (200 ng/mL) *pyocyanin*.

Additionally, the catalyst can be modified or functionalized further to improve its *pyocyanin* detection performance. Moreover, without an aptamer, TiO<sub>2</sub>-NiO-rGO cyclic voltammograms demonstrated a larger area and distinguish-

able oxidation and reduction peaks in detecting *pyocyanin*. Overall, the electrochemical detection of *pyocyanin* using a TiO<sub>2</sub>-NiO-rGO catalyst holds great potential for various applications, such as in environmental monitoring, clinical diagnostics, and drug discovery, where the detection of *pyocyanin* is of interest.

Further research and optimization of the catalyst composition, morphology, and surface modifications can contribute to advancing this electrochemical detection approach for *pyocyanin* detection. Furthermore, the electrochemical detection of *pyocyanin* using a TiO<sub>2</sub>-NiO-rGO catalyst has the potential to aid in the diagnosis and monitoring of VAP, as *pyocyanin* is a virulence factor secreted by *P. aeruginosa*, one of the main pathogens causing VAP. Developing a sensitive and selective detection method for *pyocyanin* could improve the accuracy and speed of VAP diagnosis, leading to better patient outcomes.

**Author Contributions** *Conceptualization*: Mohammad Noorizadeh, Tamim M. Al-Hasan, Mizaj S. Sha, Faycal Bensaali, Nader Meskin, Kishor K. Sadasivuni, Susu M. Zughaier, Mahmoud Elgamal, Ali Ait Hssain; *Methodology*: Mohammad Noorizadeh, Tamim M. Al-Hasan, Mizaj S. Sha, Faycal Bensaali, Nader Meskin, Kishor K. Sadasivuni, Susu M. Zughaier, Mahmoud Elgamal, Ali Ait Hssain; *Formal analysis and investigation*: Mohammad Noorizadeh, Tamim M. Al-Hasan, Mizaj S. Sha, Faycal Bensaali, Nader Meskin, Kishor K. Sadasivuni, Susu M. Zughaier, Mahmoud Elgamal, Ali Ait Hssain; *Writing — original draft preparation*: Mohammad Noorizadeh, Tamim M. Al-Hasan, Mizaj S. Sha, Mahmoud Elgamal; *Writing — review and editing*: Faycal Bensaali, Nader Meskin, Kishor K. Sadasivuni, Susu M. Zughaier, Ali Ait Hssain; *Supervision*: Faycal Bensaali, Nader Meskin, Kishor K. Sadasivuni, Susu M. Zughaier, Ali Ait Hssain; *Project administration*: Faycal Bensaali.

**Funding** This paper was supported by the International Research Collaboration Co-Fund (IRCC) grant of Qatar University under grant no. IRCC-2022-569. The findings achieved herein are solely the responsibility of the authors. Open Access funding provided by the Qatar National Library.

**Availability of data and materials** The data from this study will be made available on request.

## Declarations

**Consent for publication** All the authors approved communicating this manuscript for publication.

**Competing interests** The authors declare no competing interests.

**Open Access** This article is licensed under a Creative Commons Attribution 4.0 International License, which permits use, sharing, adaptation, distribution and reproduction in any medium or format, as long as you give appropriate credit to the original author(s) and the source, provide a link to the Creative Commons licence, and indicate if changes were made. The images or other third party material in this article are included in the article's Creative Commons licence, unless indicated otherwise in a credit line to the material. If material is not included in the article's Creative Commons licence and your



intended use is not permitted by statutory regulation or exceeds the permitted use, you will need to obtain permission directly from the copyright holder. To view a copy of this licence, visit <http://creativecommons.org/licenses/by/4.0/>.

## References

- M. Valencia, A. Torres, Ventilator-associated pneumonia. *Curr. Opin. Crit. Care* **15**(1), 30–35 (2009)
- A.S. Cooper, Oral hygiene care to prevent ventilator-associated pneumonia in critically ill patients. *Crit. Care Nurse* **41**(4), 80–82 (2021)
- J. Chastre, J.-Y. Fagon, Ventilator-associated pneumonia. *Am. J. Respir. Crit. Care Med.* **165**(7), 867–903 (2002)
- W.G. Melsen, M.M. Rovers, M. Koeman, M.J. Bonten, Estimating the attributable mortality of ventilator-associated pneumonia from randomized prevention studies. *Crit. Care Med.* **39**(12), 2736–2742 (2011)
- M.J. Richards, J.R. Edwards, D.H. Culver, R.P. Gaynes, N.N.I.S. System et al., Nosocomial infections in combined medical-surgical intensive care units in the united states. *Infection Control & Hospital Epidemiology* **21**(8), 510–515 (2000)
- Y.-Y. Chen, L.-Y. Chen, S.-Y. Lin, P. Chou, S.-Y. Liao, F.-D. Wang, Surveillance on secular trends of incidence and mortality for device-associated infection in the intensive care unit setting at a tertiary medical center in taiwan, 2000–2008: A retrospective observational study. *BMC Infect. Dis.* **12**(1), 1–11 (2012)
- J. Rello, D.A. Ollendorf, G. Oster, M. Vera-Llonch, L. Bellm, R. Redman, M.H. Kollef et al., Epidemiology and outcomes of ventilator-associated pneumonia in a large us database. *Chest* **122**(6), 2115–2121 (2002)
- L. Berra, J. Sampson, J. Wiener-Kronish, Pseudomonas aeruginosa: acute lung injury or ventilator-associated pneumonia? *Minerva Anesthesiol.* **76**(10), 824–832 (2010)
- H. Zhuo, K. Yang, S.V. Lynch, R.H. Dotson, D.V. Glidden, G. Singh, W.R. Webb, B.M. Elicker, O. Garcia, R. Brown et al., Increased mortality of ventilated patients with endotracheal pseudomonas aeruginosa without clinical signs of infection. *Crit. Care Med.* **36**(9), 2495–2503 (2008)
- L.E. Morrow, M.H. Kollef, Recognition and prevention of nosocomial pneumonia in the intensive care unit and infection control in mechanical ventilation. *Crit. Care Med.* **38**, 352–362 (2010)
- A. Rea-Neto, N.C.M. Youssef, F. Tuche, F. Brunkhorst, V.M. Ranieri, K. Reinhart, Y. Sakr, Diagnosis of ventilator-associated pneumonia: a systematic review of the literature. *Crit. Care* **12**(2), 1–14 (2008)
- J.-L. Vincent, D. Souza Barros, S. Cianferoni, Diagnosis, management and prevention of ventilator-associated pneumonia: an update. *Drugs* **70**, 1927–1944 (2010)
- J. Beyersmann, P. Gastmeier, H. Grundmann, S. Bärwolff, C. Gefers, M. Behnke, H. Rüden, M. Schumacher, Use of multistate models to assess prolongation of intensive care unit stay due to nosocomial infection. *Infection Control & Hospital Epidemiology* **27**(5), 493–499 (2006)
- E. Tejerina, A. Esteban, P. Fernández-Segoviano, F. Frutos-Vivar, J. Aramburu, D. Ballesteros, J.M. Rodríguez-Barbero, Accuracy of clinical definitions of ventilator-associated pneumonia: comparison with autopsy findings. *J. Crit. Care* **25**(1), 62–68 (2010)
- J. Rello, M. Gallego, D. Mariscal, R. Soñora, J. Valles, The value of routine microbial investigation in ventilator-associated pneumonia. *Am. J. Respir. Crit. Care Med.* **156**(1), 196–200 (1997)
- A.T. Artigas, S.B. Drona, E.C. Vallés, J.M. Marco, M.C.V. Usón, P. Figueras, F. Suarez, A. Hernandez, Risk factors for nosocomial pneumonia in critically ill trauma patients. *Crit. Care Med.* **29**(2), 304–309 (2001)
- J.-Y. Fagon, J. Chastre, M. Wolff, C. Gervais, S. Parer-Aubas, F. Stéphane, T. Similowski, A. Mercat, J.-L. Diehl, J.-P. Sollet, A. Tenaillon, for the VAP Trial Group\*, Invasive and noninvasive strategies for management of suspected ventilator-associated pneumonia. *Ann. Intern. Med.* **132**(8), 621 (2000)
- M. Leone, F. Garcin, J. Bouvenot, I. Boyadjev, P. Visintini, J. Albanèse, C. Martin, Ventilator-associated pneumonia: breaking the vicious circle of antibiotic overuse. *Crit. Care Med.* **35**(2), 379–85386 (2007)
- J. Chastre, Evolving problems with resistant pathogens. *Clin. Microbiol. Infect.* **14**(Suppl 3), 3–14 (2008)
- M.H. Kollef, Inadequate antimicrobial treatment: an important determinant of outcome for hospitalized patients. *Clin. Infect. Dis.* **31**(Supplement\_4), 131–8 (2000)
- R.H. Deurenberg, C. Vink, S. Kalenic, A.W. Friedrich, C.A. Bruggeman, E.E. Stobberingh, The molecular evolution of methicillin-resistant staphylococcus aureus. *Clin. Microbiol. Infect.* **13**(3), 222–235 (2007)
- S.K. Fridkin, J. Hageman, L.K. McDougal, J. Mohammed, W.R. Jarvis, T.M. Perl, F.C. Tenover, Vancomycin-Intermediate Staphylococcus aureus Epidemiology Study Group: Epidemiological and microbiological characterization of infections caused by staphylococcus aureus with reduced susceptibility to vancomycin, united states, 1997–2001. *Clin. Infect. Dis.* **36**(4), 429–439 (2003)
- M.M. Neuhauser, R.A. Weinstein, R. Rydman, L.H. Danziger, G. Karam, J.P. Quinn, Antibiotic resistance among gram-negative bacilli in US intensive care units: implications for fluoroquinolone use. *JAMA* **289**(7), 885–888 (2003)
- M. Macht, J.C. Robinson, B.B. Graham, Updated approach for the assessment of ventilator-associated pneumonia. *Crit. Care Med.* **41**(11), 2641–2642 (2013)
- T. Nanao, H. Nishizawa, J. Fujimoto, T. Ogawa, Additional medical costs associated with ventilator-associated pneumonia in an intensive care unit in japan. *Am. J. Infect. Control* **49**(3), 340–344 (2021)
- D.J. Anderson, K.B. Kirkland, K.S. Kaye, P.A. Thacker, Z.A. Kanafani, G. Auten, D.J. Sexton, Underresourced hospital infection control and prevention programs: penny wise, pound foolish? *Infection Control & Hospital Epidemiology* **28**(7), 767–773 (2007)
- U. Rajaji, M. Govindasamy, R. Sha, R.A. Alshgari, R.-S. Juang, T.-Y. Liu, Surface engineering of 3d spinel zn<sub>3</sub>v<sub>2</sub>o<sub>8</sub> wrapped on sulfur doped graphitic nitride composites: Investigation on the dual role of electrocatalyst for simultaneous detection of antibiotic drugs in biological fluids. *Compos. B Eng.* **242**, 110017 (2022). <https://doi.org/10.1016/j.compositesb.2022.110017>
- U. Rajaji, S.V. Selvi, S.-M. Chen, S. Chinnapaiyan, T.-W. Chen, M. Govindasamy, A nanocomposite consisting of cuprous oxide supported on graphitic carbon nitride nanosheets for non-enzymatic electrochemical sensing of 8-hydroxy-2-deoxyguanosine. *Microchimica Acta* **187**(8) (2020). <https://doi.org/10.1007/s00604-020-04416-2>
- W. Khushaim, V. Mani, K. Peramaiya, K.-W. Huang, K.N. Salama, Ruthenium and nickel molybdate-decorated 2d porous graphitic carbon nitrides for highly sensitive cardiac troponin biosensor. *Biosensors* **12**, (10) (2022). <https://doi.org/10.3390/bios12100783>
- U. Rajaji, M.S. Raghu, K. Yogesh Kumar, T.M. Almutairi, A.A. Mohammed, R.-S. Juang, T.-Y. Liu, A sonochemical synthesis of rtio<sub>3</sub> supported n-doped graphene oxide as a highly efficient electrocatalyst for electrochemical reduction of a chemotherapeutic drug. *Ultrason. Sonochem.* **93**, 106293 (2023). <https://doi.org/10.1016/j.ultrsonch.2023.106293>
- J.W. Gardner, P.N. Bartlett, A brief history of electronic noses. *Sens. Actuators, B Chem.* **18**(1–3), 210–211 (1994)

32. C.-Y. Chen, W.-C. Lin, H.-Y. Yang, Diagnosis of ventilator-associated pneumonia using electronic nose sensor array signals: solutions to improve the application of machine learning in respiratory research. *Respir. Res.* **21**(1), 1–12 (2020)
33. R. Schnabel, M. Boumans, A. Smolinska, E. Stobberingh, R. Kaufmann, P. Roekaerts, D. Bergmans, Electronic nose analysis of exhaled breath to diagnose ventilator-associated pneumonia. *Respir. Med.* **109**(11), 1454–1459 (2015)
34. S.G. Armato, M.L. Giger, C.J. Moran, J.T. Blackburn, K. Doi, H. MacMahon, Computerized detection of pulmonary nodules on ct scans. *Radiographics* **19**(5), 1303–1311 (1999)
35. Y. Yim, H. Hong, Y.G. Shin, Hybrid lung segmentation in chest ct images for computer-aided diagnosis. In: Proceedings of 7th International Workshop on Enterprise Networking and Computing in Healthcare Industry, 2005. HEALTHCOM 2005., IEEE, pp. 378–383 (2005)
36. J. Pu, J. Roos, A.Y. Chin, S. Napel, G.D. Rubin, D.S. Paik, Adaptive border marching algorithm: automatic lung segmentation on chest ct images. *Comput. Med. Imaging Graph.* **32**(6), 452–462 (2008)
37. Y. Gu, V. Kumar, L.O. Hall, D.B. Goldgof, C.-Y. Li, R. Korn, C. Bendtsen, E.R. Velazquez, A. Dekker, H. Aerts et al., Automated delineation of lung tumors from ct images using a single click ensemble segmentation approach. *Pattern Recogn.* **46**(3), 692–702 (2013)
38. N. Shafran, I. Shafran, H. Ben-Zvi, S. Sofer, L. Sheena, I. Krause, A. Shlomai, E. Goldberg, E.H. Sklan, Secondary bacterial infection in covid-19 patients is a stronger predictor for death compared to influenza patients. *Sci. Rep.* **11**(1), 12703 (2021)
39. B. Kaçmaz, Ş Keske, U. Şişman, S.T. Ateş, M. Güldan, Y. Beşli, E. Palaoğlu, N. Çakar, Ö. Ergönül, Covid-19 associated bacterial infections in intensive care unit: a case control study. *Sci. Rep.* **13**(1), 13345 (2023)
40. V. De Santis, A. Corona, D. Vitale, C. Nencini, A. Potalivo, A. Prete, G. Zani, A. Malfatto, L. Tritapepe, S. Taddei et al, Bacterial infections in critically ill patients with sars-2-covid-19 infection: results of a prospective observational multicenter study. *Infection*, pp. 1–10 (2021)
41. G. Seo, G. Lee, M.J. Kim, S.-H. Baek, M. Choi, K.B. Ku, C.-S. Lee, S. Jun, D. Park, H.G. Kim et al., Rapid detection of covid-19 causative virus (sars-cov-2) in human nasopharyngeal swab specimens using field-effect transistor-based biosensor. *ACS Nano* **14**(4), 5135–5142 (2020)
42. X. Zhang, Q. Qi, Q. Jing, S. Ao, Z. Zhang, M. Ding, M. Wu, K. Liu, W. Wang, Y. Ling et al, Electrical probing of covid-19 spike protein receptor binding domain via a graphene field-effect transistor, (2020). arXiv preprint [arXiv:2003.12529](https://arxiv.org/abs/2003.12529)
43. H. Chen, T.K. Choo, J. Huang, Y. Wang, Y. Liu, M. Platt, A. Palaniappan, B. Liedberg, A.I.Y. Tok, Label-free electronic detection of interleukin-6 using horizontally aligned carbon nanotubes. *Materials & Design* **90**, 852–857 (2016)
44. D. Gentili, P. D'Angelo, F. Militano, R. Mazzei, T. Poerio, M. Brucale, G. Tarabella, S. Bonetti, S.L. Marasso, M. Cocuzza et al, Integration of organic electrochemical transistors and immunaffinity membranes for label-free detection of interleukin-6 in the physiological concentration range through antibody–antigen recognition. *Journal of Materials Chemistry B* **6**(33), 5400–5406 (2018)
45. Z. Hao, Y. Pan, W. Shao, Q. Lin, X. Zhao, Graphene-based fully integrated portable nanosensing system for on-line detection of cytokine biomarkers in saliva. *Biosens. Bioelectron.* **134**, 16–23 (2019)
46. C. Chan, J. Shi, Y. Fan, M. Yang, A microfluidic flow-through chip integrated with reduced graphene oxide transistor for influenza virus gene detection. *Sens. Actuators, B Chem.* **251**, 927–933 (2017)
47. Y.-J. Chen, C.-L. Chiang, J.-T. Huang, Wireless portable graphene-fet biosensor for detecting h1n1 virus. *Cancer* **176**, 9 (2010)
48. T. Ono, T. Oe, Y. Kanai, T. Ikuta, Y. Ohno, K. Maehashi, K. Inoue, Y. Watanabe, S.-I. Nakakita, Y. Suzuki et al., Glycan-functionalized graphene-fets toward selective detection of human-infectious avian influenza virus. *Jpn. J. Appl. Phys.* **56**(3), 030302 (2017)
49. T.A. Webster, H.J. Sismaet, J.L. Conte, E.D. Goluch et al., Electrochemical detection of pseudomonas aeruginosa in human fluid samples via pyocyanin. *Biosens. Bioelectron.* **60**, 265–270 (2014)
50. F. Jia, E. Barber, H. Turasan, S. Seo, R. Dai, L. Liu, X. Li, A.K. Bhunia, J.L. Kokini, Detection of pyocyanin using a new biodegradable sers biosensor fabricated using gold coated zein nanostructures further decorated with gold nanoparticles. *J. Agric. Food Chem.* **67**(16), 4603–4610 (2019). <https://doi.org/10.1021/acs.jafc.8b07317>. PMID: 30964288
51. F.A. Alatraktchi, J.S. Noori, G.P. Tanev, J. Mortensen, M. Dimaki, H.K. Johansen, J. Madsen, S. Molin, W.E. Svendsen, Paper-based sensors for rapid detection of virulence factor produced by pseudomonas aeruginosa. *PLoS ONE* **13**(3), 0194157 (2018)
52. X. Wu, J. Chen, X. Li, Y. Zhao, S.M. Zughair, Culture-free diagnostics of pseudomonas aeruginosa infection by silver nanorod array based sers from clinical sputum samples. *Nanomedicine: Nanotechnology, Biology and Medicine* **10**(8), 1863–1870 (2014)
53. F.A. Alatraktchi, W.E. Svendsen, S. Molin, Electrochemical detection of pyocyanin as a biomarker for pseudomonas aeruginosa: A focused review. *Sensors* **20**(18), 5218 (2020)
54. A.A. Elkhawaga, M.M. Khalifa, O. El-Badawy, M.A. Hassan, W.A. El-Said, Rapid and highly sensitive detection of pyocyanin biomarker in different pseudomonas aeruginosa infections using gold nanoparticles modified sensor. *PLoS ONE* **14**(7), 0216438 (2019)
55. S. Mukherjee, S. Su, W. Panmanee, R.T. Irvin, D.J. Hassett, S. Choi, A microliter-scale microbial fuel cell array for bacterial electrogenic screening. *Sens. Actuators, A* **201**, 532–537 (2013). <https://doi.org/10.1016/j.sna.2012.10.025>
56. S.N. Alam, N. Sharma, L. Kumar, Synthesis of graphene oxide (go) by modified hummers method and its thermal reduction to obtain reduced graphene oxide (rgo). *Graphene* **6**(1), 1–18 (2017)
57. M.S. Sha, F. N. Musthafa, A. Alejli, J.K. Alahmad, B. Bhattacharyya, B. Kumar, A.M. Abdullah, K.K. Sadasivuni, An advanced quaternary composite for efficient water splitting. *Catalysis Letters* (2023). <https://doi.org/10.1007/s10562-023-04339-6>
58. B. Muthukutty, T.C. Doan, H. Yoo, Binary metal oxide (nio/sno2) composite with electrochemical bifunction: Detection of neuro transmitting drug and catalysis for hydrogen evolution reaction. *Environ. Res.* **241**, 117655 (2024). <https://doi.org/10.1016/j.envres.2023.117655>
59. V.L.E. Siong, K.M. Lee, J.C. Juan, C.W. Lai, X.H. Tai, C.S. Khe, Removal of methylene blue dye by solvothermally reduced graphene oxide: a metal-free adsorption and photodegradation method. *RSC Adv.* **9**, 37686–37695 (2019). <https://doi.org/10.1039/C9RA05793E>
60. P. Kumar, N. Divya, J.K. Ratan, Study on the physico-chemical properties of reduced graphene oxide with different degrees of reduction temperature. *J. Iran. Chem. Soc.* **18**(1), 201–211 (2020). <https://doi.org/10.1007/s13738-020-02014-w>
61. M.R. Thalji, G.A.M. Ali, P. Liu, Y.L. Zhong, K.F. Chong, W18o49 nanowires-graphene nanocomposite for asymmetric supercapacitors employing alc3 aqueous electrolyte. *Chem. Eng. J.* **409**, 128216 (2021). <https://doi.org/10.1016/j.cej.2020.128216>
62. C. McLean, K. Brown, J. Windmill, L. Dennany, Innovations in point-of-care electrochemical detection of pyocyanin. *J. Electroanal. Chem.* **921**, 116649 (2022). <https://doi.org/10.1016/j.jelechem.2022.116649>

## Authors and Affiliations

Mohammad Noorizadeh<sup>1</sup> · Tamim M. Al-Hasan<sup>1</sup> · Mizaj S. Sha<sup>2</sup> · Faycal Bensaali<sup>1</sup> · Nader Meskin<sup>1</sup> · Kishor K. Sadasivuni<sup>2</sup> · Susu M. Zughaier<sup>3</sup> · Mahmoud Elgamal<sup>3</sup> · Ali Ait Hssain<sup>4</sup>

Tamim M. Al-Hasan  
tm1800463@qu.edu.qa

Mizaj S. Sha  
misajmisfa@gmail.com

Faycal Bensaali  
f.bensaali@qu.edu.qa

Nader Meskin  
nader.meskin@qu.edu.qa

Kishor K. Sadasivuni  
kishorkumars@qu.edu.qa

Susu M. Zughaier  
szughaier@qu.edu.qa

Mahmoud Elgamal  
mahmoud.elgamal@qu.edu.qa

Ali Ait Hssain  
AHssain@hamad.qa

<sup>1</sup> Department of Electrical Engineering, College of Engineering, Qatar University, Doha, Qatar

<sup>2</sup> Center for Advanced Material, Research Complex, Qatar University, Doha, Qatar

<sup>3</sup> College of Medicine, Qatar University, Doha, Qatar

<sup>4</sup> Medical Intensive Care Unit, Hamad Medical Corporation, Doha, Qatar